Oil Spill Detection via Multitemporal Optical Remote Sensing Images: A Change Detection Perspective

Sicong Liu, *Member, IEEE*, Mingmin Chi, *Member, IEEE*, Yangxiu Zou, Alim Samat, *Member, IEEE*, Jón Atli Benediktsson, *Fellow, IEEE*, and Antonio Plaza, *Fellow, IEEE*

***Abstract*— Oil spill monitoring in optical remote sensing (RS) images is a challenging task due to the complexity of target discrimination in an oil spill scenario. Differently from traditional oil spill detection methods that are mainly carried out in a monotemporal image, in this letter, a novel solution is given in a multitemporal domain by investigating potential capability of change detection (CD) techniques, and it mainly contributes to an unsupervised, semiautomatic, and efficient approach. It opens a new perspective for solving an oil spill detection problem. In particular, a coarse-to-fine multitemporal change analysis procedure is designed to investigate the spectral–temporal variation of change targets present in the scenario. Changes relevant and irrelevant to suspected oil spills are identified and discriminated according to a binary and a multiple CD process, respectively. The proposed approach provides a quick yet effective oil spill detection solution, which is valuable and important in practical applications. The proposed method was validated on two real multitemporal RS data sets presenting the oil spill event in northern Gulf of Mexico in 2010. Experimental results confirmed its effectiveness.**

***Index Terms*— Change detection (CD), change vector analysis, coarse-to-fine (CTF), multitemporal data, oil spill, optical remote sensing (RS).**

I. Introduction

OIL pollution is an increasingly critical ocean disaster over the world, attracting significant attention on this topic. It may result from different sources, for example, urban runoff and industrial discharges, oil production, particle settlement in the atmosphere, natural oil seepage, and tanker accidents [1]. Negative effects of oil spills are related to marine and coastal environment, marine exploration, transportation, and so on, at both regional and global levels [2]. Therefore, it is very urgent and important to effectively detect oil spills on ocean surface in time, in order to facilitate government decision making and scientific research at next stage.

Thanks to the revisit time, wide area coverage, and relatively low cost properties, satellite remote sensing (RS) is playing an increasingly important role in oil spill monitoring. Space-borne oil spill detection can complement and optimize the traditional *in situ* investigation, which is difficult and even impossible to manage in time. RS techniques have been widely used in oil spill monitoring in the past decades [1]–[3]. Among different sensors mounted on satellites, active microwave instruments (e.g., synthetic aperture radar) and its corresponding analysis techniques have been frequently investigated for oil monitoring in [4] and [5]. Microwave sensors have all-weather and all-day capabilities for Earth observation. Microwave backscattering properties of ocean surfaces are directly reflected on image brightness, and thus they are commonly utilized in identifying oil-like features. However, the use of microwave sensors is limited by their high cost, relatively small swath widths, and low revisit frequencies [1]. Open issues such as estimation of the thickness of oil spills and recognition of oil types are still unsolved.

Although passive optical sensor images may be contaminated by clouds, compared with microwave sensors, they have unique characteristic to measure oil slicks from the spectrum point of view. Open issues aforementioned for microwave sensor images might be addressed in optical images by exploring in detail spectral behaviors. Therefore, optical multispectral images are potentially capable to identify oil spills at a fine level. Several works have attempted to explore such potential capability in oil spill detection [1], [6]–[10]. Most of them are designed based on the single-time oil spill image and are devoted to locating the position of oil spills. We can group them into two main categories: 1) qualitative manual inspection-based approaches, e.g., analyzing the derived index images and enhancing the oil–water contrast [1], [6]–[8] and 2) automatic detection methods based on supervised classifiers [9], [10]. The former does not require ground reference data; however, it does not allow a quantitative evaluation. The latter is carried out relying on the available ground reference samples to train a supervised classifier. A fine and

Manuscript received July 21, 2016; revised September 26, 2016 and December 7, 2016; accepted December 7, 2016. Date of publication January 26, 2017; date of current version February 23, 2017. This work was supported in part by the Natural Science Foundation of China under Grant 41601354 and Grant 41601440, in part by the Open Foundation of Second Institute of Oceanography under Contract SOED1509, and in part by the Dragon 3 Program sponsored by the Ministry of Science and Technology of China and the European Space Agency under Contract 10689. *(Correspondence author: Mingmin Chi.)*

S. Liu is with the College of Surveying and Geoinformatics, Tongji University, Shanghai 200092, China (e-mail: sicongliu.rs@gmail.com).

M. Chi and Y. Zou are with the Shanghai Key Laboratory of Data Science, Key Laboratory for Information Science of Electromagnetic Waves, School of Computer Science, Fudan University, Shanghai 201203, China, and also with the State Key Laboratory of Satellite Ocean Environment Dynamics, Second Institute of Oceanography, Hangzhou 310012, China (e-mail: mmchi@fudan.edu.cn).

A. Samat is with the State Key Laboratory of Desert and Oasis Ecology, Xinjiang Institute of Ecology and Geography, CAS, Urumqi 830011, China.

J. A. Benediktsson is with the Faculty of Electrical and Computer Engineering, University of Iceland, IS-107 Reykjavik, Iceland.

A. Plaza is with the Department of Technology of Computers and Communications, University of Extremadura, E-10071 Caceres, Spain.

Color versions of one or more of the figures in this letter are available online at http://ieeexplore.ieee.org.

Digital Object Identifier 10.1109/LGRS.2016.2639540

automatic identification of oil spills and discrimination among look-alikes (e.g., algal blooms, clouds, sun glints) are required to be further investigated.

In this letter, a novel coarse-to-fine (CTF) oil spill detection approach is designed. It is suitable for locating oil spills and is potentially capable for discriminating suspected oil spill relevant and irrelevant targets in a large scenario. In particular, the original oil spill detection task in a monotemporal domain is converted into a change detection (CD) task that is solved in a multitemporal domain. The proposed CTF technique allows a quick discovery of the suspected oil spills while investigating quantitatively the detailed information inside. For users do not have any prior knowledge on the data set and scenario, the proposed technique provides an effective tool for oil spill mining, discovery, and detection, especially for locating the "target" regions having a high probability related to oil spills. The proposed method is validated on two medium-resolution optical satellite data sets (i.e., HJ-1 and Landsat) associated with the oil spill event on April 20, 2010, in northern Gulf of Mexico (GOM). Experimental results confirm the effectiveness of the proposed technique for a quick and fine oil spill detection.

The remainder of this letter is organized as follows. Section II analyzes and discusses oil spill detection in monotemporal and multitemporal images, respectively. Section III presents the proposed CTF approach. Section IV describes two used data sets, analyzes, and discusses the experimental results. The final conclusion is given in Section V.

II. Oil Spill Detection in Monotemporal and Multitemporal Images

The visibility of an oil spill is mainly due to the quality of image (e.g., clouds contamination, noise distribution) and the optical contrast between spills and the surrounding water in both monotemporal and multitemporal image domains. For the oil–water contrast, two conditions might be observed [8]: 1) glint, i.e., positive contrast, oil brighter than water and 2) glint-free, i.e., negative contrast, oil darker than water. Several works were devoted to distinguishing these two conditions in optical images [6], [8]. In this paper, we focus on the former.

In a monotemporal image domain, the aim of oil spill detection is to extract the target (i.e., oil spills) from the background (i.e., sea water), which may contain many irrelevant targets (e.g., algal blooms, clouds, and sun glint areas). To this end, the considered oil spill detection problem can be addressed either according to qualitative manual inspection or quantitative classification as summarized in Section I. Note that the oil spill detection performance in a monotemporal image depends on the class separability between oil slicks and irrelevant targets. In reality, oil spill features might not be explicitly identified due to the insignificant oil–water contrast. Thus an automatic separation is difficult to be realized due to the presence of similar spectral properties in oil slicks and water. Moreover, a probably high number of irrelevant targets in the scenario may make this task more complex and challenging, especially in an unsupervised way.

On the contrary, analysis of multitemporal images may open a new perspective for oil spill detection in a more robust and precise way. In RS, CD is designed for identifying changes occurred in a geographical area at different observation times [11]. CD techniques have been widely used in different RS applications; however, advantages of such techniques have not been investigated for oil spill monitoring, especially in optical images. In a multitemporal domain, oil spills are expected to be detected as a change class that can be discriminated from an unchanged background (i.e., sea) and irrelevant changes (e.g., presence/absence of other targets). Spectral–temporal variations of oil spills and irrelevant targets have different spectral significance. Thus, oil spills are more likely to be detected in a multitemporal domain.

III. Proposed Coarse-To-Fine Change Analysis Approach for Oil Spill Detection

Let $\mathbf{X}_1$ be a selected "base" image in a data archive, which is oil-free, and $\mathbf{X}_2$ be an input image acquired over the same scenario for detecting suspected oil spills. $\mathbf{X}_2$ is coregistered to $\mathbf{X}_1$. Let $\Omega = \{\omega_n, \Omega_c\}$ be the set of all classes present in the scenario in the multitemporal domain, ω_n be the no-change sea background and $\Omega_c = \{\omega_{C_1}, \omega_{C_2}, \ldots, \omega_{C_K}\}$ be the set of K possible change targets. The considered oil spill detection can be formalized as a problem to isolate a set of oil relevant changes $\Omega_{c,O}$ in Ω_c ($\Omega_{c,O} \in \Omega_c$) from the oil-irrelevant changes $\Omega_{c,N}$ (e.g., algal blooms, ships, etc.) and the no-change class ω_n. $\Omega_{c,N} \in \Omega_c$, $\Omega_c = \{\Omega_{c,O}, \Omega_{c,N}\}$. A novel CTF approach is proposed to discover and detect suspected oil spills in multitemporal images from global to local scales by following a binary-to-multiple CD procedure. Block scheme of the proposed approach is illustrated in Fig. 1. It mainly consists of three steps: 1) multitemporal image preprocessing; 2) coarse oil spill change analysis; and 3) fine oil spill change analysis. Details of each step are given as follows.

A. Multitemporal Images Preprocessing

Due to the fact that oil spills only exist on the sea surface, it is necessary to mask land regions that may contain a large portion of oil irrelevant changes. Moreover, changes that are caused by the absence or presence of clouds may affect the detection of oil spills, so clouds are also masked on each image. This not only reduces the unnecessary change analysis and the resulting computational cost, but also enhances oil spill visualization and identification on the sea surface. To mask land regions, Normalized Difference Vegetation Index (NDVI) result of each single date image is segmented according to a predefined threshold $T_I = 0$. NDVI value indicates the highest possible density of green leaves like vegetation (close to 1), or water, cloud, and snow (close to -1). Segmentation on NDVI is sufficient and especially fast for a binary separation between the sea ($<T_I$) and the land ($\geqslant T_I$). An improved background suppressed haze thickness index method [12] is applied to detect clouds, which are removed from two images. Note that the masking operations are automatic without the requirement of any assistance of manual work or reference samples.

B. Coarse Oil Spill Change Analysis

In this step, a coarse oil spill detection is conducted at a global scale. The objective is to locate all possible targets

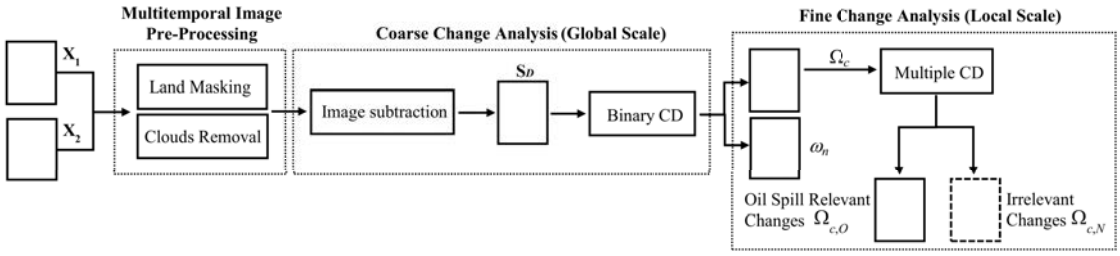

Fig. 1. Block scheme of the proposed CTF oil spill detection technique.

presented on the sea surface while separating them from the sea background. This is solved as a binary CD task in the multitemporal domain to separate the change (i.e., Ω_c) and no-change (i.e., ω_n) classes. Two geo-referenced and masked images are compared to find pixels without masked in both images. These pixels are extracted for further computation. Let $\mathbf{S}_1$ and $\mathbf{S}_2$ be the selected subset of pixels for CD from $\mathbf{X}_1$ and $\mathbf{X}_2$, respectively. $\mathbf{S}_D$ is the set of spectral change vectors (SCVs) defined as

$$\mathbf{S}_D = \mathbf{S}_2 - \mathbf{S}_1. \tag{1}$$

Change magnitude ρ is then defined by calculating the Euclidean compression of SCVs in (1), which indicates a probability of a pixel being change or no change according to its magnitude value. It is defined as

$$\rho = \sqrt{\sum_{b=1}^{B} (\mathbf{S}_{D,b})^2} \tag{2}$$

where $\mathbf{S}_{D,b}$ is the bth ($b = 1, \ldots, B$) component of $\mathbf{S}_D$, and B is the number of spectral channels in the considered images.

Automatic techniques such as thresholding and clustering can be utilized to address a binary CD problem. In this paper, a threshold T_ρ is defined by using an improved Kittler and Illingworth (KI) minimum-error thresholding algorithm [13] for segmenting all pixels in $\mathbf{S}_D$ into Ω_c and ω_n two classes. Note that the extracted change targets include the suspected oil spill-relevant changes (i.e., $\Omega_{c,O}$) and irrelevant changes (i.e., $\Omega_{c,N}$), which are impossible to be further distinguished relying only on the coarse binary change analysis in this step.

C. Fine Oil Spill Change Analysis

In this step, suspected oil spill-relevant changes (i.e., $\Omega_{c,O}$) are detected at a local scale (i.e., only the pixels identified as Ω_c in the previous step are considered), separating from the irrelevant changes (i.e., $\Omega_{c,N}$) according to a multiple CD. It is challenging, in particular, in an unsupervised way. Many issues should be addressed inside, such as estimation of the number of changes, distinguishing different kinds of changes, etc. A sequential spectral change vector analysis (S^2CVA) approach [14] is applied to this end. It is recently proposed for detecting multiple changes in multitemporal hyperspectral images while exploring a hierarchical nature of complex multiple changes. It provides a quick yet effective tool for solving the aforementioned problems simultaneously in a 2-D compressed feature space. The 2-D representation is constructed based on two variables, i.e., change magnitude ρ and change direction α, to illustrate and detect multiple changes. In particular, ρ is defined as the same in (2), and α is defined as follows [14]:

$$\alpha = \text{across}\left[\left(\sum_{b=1}^{B}(\mathbf{S}_{D,b}\mathbf{r}_b) \Big/ \sqrt{\sum_{b=1}^{B}(\mathbf{S}_{D,b})^2 \sum_{b=1}^{B}(\mathbf{r}_b)^2}\right)\right] \tag{3}$$

where r_b is the bth ($b = 1, \ldots, B$) component of reference vector $\mathbf{r}$

$$\mathbf{A} = \text{cov}(\mathbf{S}_D) = E[(\mathbf{S}_D - E[\mathbf{S}_D])(\mathbf{S}_D - E[\mathbf{S}_D])^T] \tag{4}$$

where $\boldsymbol{E}[\mathbf{S}_\mathrm{D}]$ is the expectation of $\mathbf{S}_\mathrm{D}$. The eigen-decomposition of $\mathbf{A}$ can be represented as

$$\mathbf{A} \cdot \mathbf{V} = \mathbf{V} \cdot \mathbf{W} \tag{5}$$

where $\mathbf{W}$ and $\mathbf{V}$ are the matrix of eigenvalues and eigenvectors, respectively. The reference vector $\mathbf{r}$ is computed as the first eigenvector in $\mathbf{V}$ corresponding to the largest eigenvalue, which projects the original SCVs into a direction that measures maximum variance of data, thus representing different changes.

The 2-D representation in a polar domain D is defined as

$$D = \{\rho \in [0, \rho^{\max}] \text{ and } \alpha \in [0, \pi]\} \tag{6}$$

where $\rho^{\max}$ is the maximum value of ρ. The considered multiple CD problem is solved by discriminating different homogenous changes along the direction α in a sequence of domains following a hierarchical analysis [14]. Note that in the oil spill detection case when multispectral images are considered, detection at first level of the hierarchy is sufficient for identifying the major changes.

Although the change direction α is capable of separating oil spill-relevant and -irrelevant changes, it is still difficult to discriminate changes in $\Omega_{c,O}$ that are probably related to the oil spill thickness or oil–water mixture degree, due to the fact that they present almost the same direction α, especially in a multispectral case with limited spectral bands. Difference information is actually present in the magnitude of $\Omega_{c,O}$, which has not been finely investigated in the previous step. Therefore, an additional change analysis is implemented iteratively on the magnitudes of SCVs belonging to $\Omega_{c,O}$. Both hard and soft oil spill detection results are obtained, representing the different information in the extracted $\Omega_{c,O}$. The hard detection result is generated by interactively defining thresholds according to modes on the magnitude histogram. Thus different change classes are separated in $\Omega_{c,O}$. A soft oil spill detection result can be generated by illustrating pixels in pseudocolor without defining classes as in the hard decision. Different pseudocolors indicate possible different

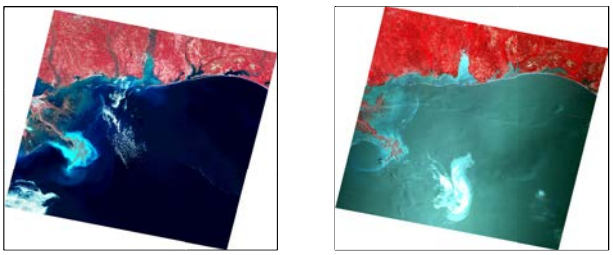

Fig. 2. False color composite (R:b4, G:b3, B:b2) of HJ-1 images over GOM acquired in (a) 2009 ($\mathbf{X}_1$) and (b) 2010 ($\mathbf{X}_2$).

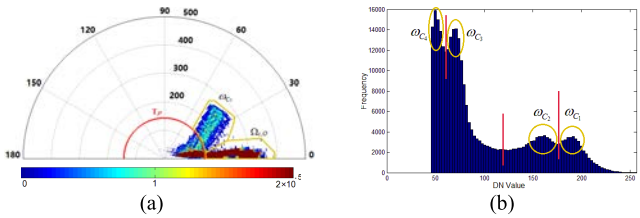

Fig. 3. (a) 2-D change representation by the adaptive SCV analysis approach [15]. (b) Magnitude histogram of the oil relevant change $\Omega_{c,O}$.

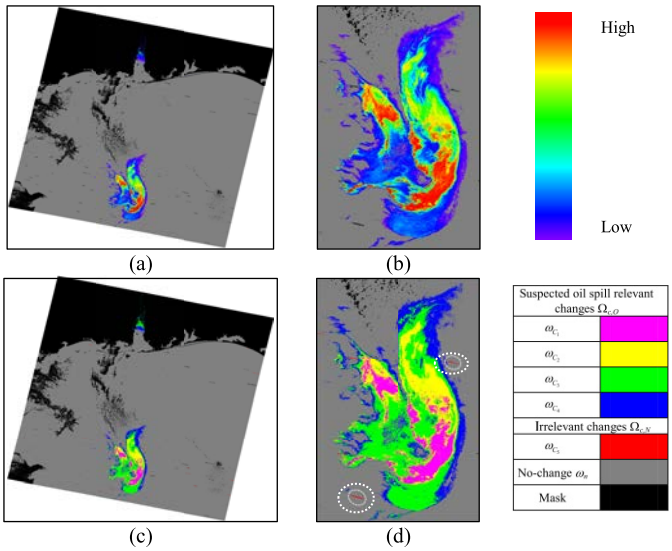

Fig. 4. Oil spill detection results obtained by the proposed CTF approach (HJ-1 data set). (a) Soft detection. (b) Subset of (a). (c) Hard detection. (d) Subset of (c).

oil spill changes and change significance levels according to magnitude values. Due to the unsupervised nature of the proposed approach and with the limited spectral representation in a multispectral case, it is impossible to accurately identify specific types of oil spills without prior knowledge. However, the proposed approach narrows the oil spill searching range down in a large scenario and provides a quick solution to locate and discriminate suspected oil spills by analyzing pixel spectral–temporal behaviors. This is essentially valuable in practical applications.

IV. Experimental Results

A. HJ-1 Data Set

The first data set is made up of bitemporal multispectral HJ-1A/B CCD1 images, acquired on January 9, 2009 ($\mathbf{X}_1$), and May 10, 2010 ($\mathbf{X}_2$), respectively, over the northwestern GOM. The original images contain red, green, blue, and near-infrared four bands with a spatial resolution of 30 m. Preprocessed (e.g., bands stacking, atmospheric correction) images were coregistered, with a residual error limited within 0.5 pixel. Fig. 2(a) and (b) shows the false color composite images $\mathbf{X}_1$ and $\mathbf{X}_2$, respectively.

Qualitative and quantitative analyses were carried out to evaluate the performance of the proposed approach. 2-D representation obtained by using the S^2CVA approach [14] is illustrated in Fig. 3(a). Here, the threshold T_ρ was defined to 136 [cf. the red semicircle in Fig. 3(a)] and discrimination boundaries for multiple changes were defined as yellow polygons. Oil spill relevant changes clustered at a low-value direction [cf. the cluster $\Omega_{c,O}$ in Fig. 3(a)], whereas irrelevant change ω_{C_5} is not. Magnitude histogram of $\Omega_{c,O}$ is further analyzed. In this case, four modes were identified inside $\Omega_{c,O}$, where three thresholds were interactively defined to segment four classes, i.e., ω_{C_1}-ω_{C_4} [cf. Fig. 3(b)]. Both soft and hard detection results are provided in Fig. 4(a) and (c), respectively. A subset is extracted for a better visual comparison [cf. Fig. 4(b) and (d)]. The pseudocolor in the soft detection result indicates different oil spill changes in $\Omega_{c,O}$, and is visually consistent with the obtained hard detection result based on histogram segmentation as shown in Fig. 3(b). In this case, ω_{C_5} is mainly caused by several stripe noises present in the original image bands [e.g., dotted circles highlighted in Fig. 4(d)]. According to a carefully qualitative evaluation, we can see that suspected oil spills have been successfully located and finely identified in the obtained soft and hard detection results, by following the proposed CTF approach in the multitemporal framework. In practical applications, these suspected regions are quickly locked as "target" regions for further investigation.

Quantitative analysis was made by comparing the binary oil spill detection results obtained by the proposed unsupervised CTF approach and by the supervised support vector machine (SVM) classifier [15] in the masked monotemporal image $\mathbf{S}_2$. Two-class samples were selected in $\mathbf{S}_2$ according to a carefully image interpretation, including 43 824 pixels as oil spill class and 117 626 pixels as background class, where 40% was used for training SVM and 60% for testing. Note that the SVM training and prediction were implemented in LibSVM [16] with a RBF kernel, and a grid-search and five-fold cross-validation strategy to find out the optimal parameters. The accuracy and error indices are listed in Table I; we can see that the proposed CTF approach resulted in a significant improvement on the overall accuracy (*OA*) (i.e., 92.67%) and *Kappa* (i.e., 0.8131) than SVM (i.e., 90.81% and 0.7835) in locating oil spills, especially in decreasing commission errors from 25.49% to 17.34%. Moreover, the proposed CTF approach is much computationally efficient than SVM, which only took, in total, 258.62 s to complete the whole detection at such large image scenario, whereas in the same case, SVM required 491.14 s.

B. Landsat Data Set

The second data set is a pair of multispectral Landsat ETM+ images acquired on March 30 ($\mathbf{X}_1$), and May 1 ($\mathbf{X}_2$), 2010, respectively, over the northern GOM. Bands 1–5 and 7 were selected, having a spatial resolution of 30 m. Preprocessed (e.g., band stripe repairing, atmospheric

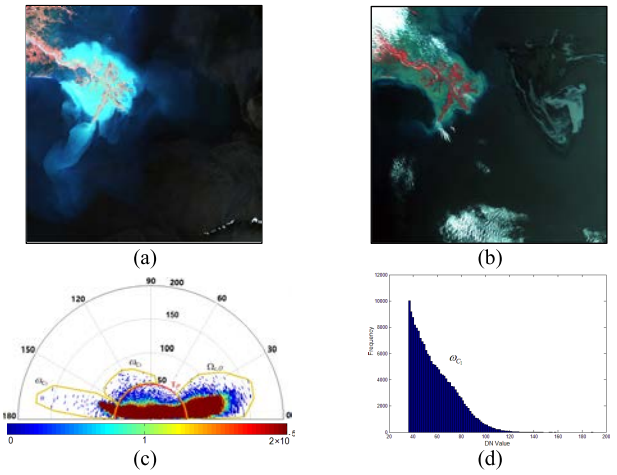

Fig. 5. False color composite (R:b4, G:b3, B:b2) of Landsat images over GOM, acquired in (a) March 2010 (**X**1) and (b) May 2010 (**X**2). (c) Obtained 2-D change representation. (d) Magnitude histogram of oil relevant change $\Omega_{c,O}$.

TABLE I

ACCURACY INDICES AND TIME COST OBTAINED BY SVM AND PROPOSED CTF APPROACH IN LOCATING OIL SPILLS

Data Set	Method	OA (%)	*Kappa*	Omission (%)	Commission (%)	Time cost (s)
HJ-1	SVM	90.81	0.7835	13.55	25.49	491.14
	CTF	92.67	0.8131	16.58	17.34	258.62
Landsat	SVM	97.42	0.9048	3.26	12.27	1138.07
	CTF	97.97	0.9191	2.80	12.50	301.15

correction) two images was coregistered with a residual error of less than 0.5 pixel. False color composite of $\mathbf{X}_1$ and $\mathbf{X}_2$ is shown in Fig. 5(a) and (b), respectively. The same experimental setup was used as in the previous case. Qualitative and quantitative analyses were conducted. The 2-D change representation is illustrated in Fig. 5(c). In the coarse binary detection,T_ρ was defined equal to 49.2, and three clusters were identified, including $\Omega_{c,O}$ and two irrelevant changes (i.e., ω_{C_2} and ω_{C_3} represent two off-shore sea water changes shown in green and red, respectively.). Note that only a single mode is represented [cf. Fig. 5(d)] in the magnitude of $\Omega_{c,O}$. It indicates a relatively homogenous oil spill spread on the sea surface. Accordingly, a single oil spill class ω_{C_1} is defined in the hard detection result. However, different information can be still observed in the pseudocolor soft detection result. Satisfactory results are qualitatively evaluated by locating oil spills and discriminating them from other targets. 139 236 pixels (oil spill class) and 632 076 pixels (background class) were selected in $\mathbf{S}_2$ as reference samples (with 40% for training, 60% for testing) in SVM. Based on a quantitative analysis of accuracies listed in Table I, one can see that the proposed CTF approach outperforms SVM, with respect to higher *OA* and *Kappa* values (i.e., 97.97% and 0.9191). Note that the computation cost in the proposed CTF approach (i.e., 301.15 s) is much less than in SVM (i.e., 1138.07 s), indicating its effectiveness in applying to a large image scenario.

V. CONCLUSION

This letter presents a new solution to the challenging oil spill detection task in a multitemporal domain. A novel CTF approach is proposed to realize a sophisticated oil spill discovery and detection at a large-scale scenario. The proposed technique is unsupervised and semiautomatic, without the availability of ground reference data, and in particular cost-efficient. Main contributions of this work include: 1) it opens a new perspective to solving the considered oil spill detection problem from a systematic CD perspective in a multitemporal domain, which has not been studied in literature according to our knowledge. Suspected oil spills are extracted and discriminated in a coarse binary and a fine multiple CD step, respectively, by investigating in details the spectral-temporal variation and 2) it detects oil spills while providing valuable soft and hard detection results. Information might associate with the oil thickness was discovered, which is not easily detectable in the popular monotemporal techniques. Experimental results confirm the effectiveness of the proposed approach. For future developments, oil spill-relevant features will be extracted to optimize the proposed technique.

REFERENCES

[1] J. Zhao, M. Temimi, H. Ghedira, and C. Hu, "Exploring the potential of optical remote sensing for oil spill detection in shallow coastal waters—A case study in the Arabian Gulf," *Opt. Exp.*, vol. 22, no. 11, pp. 13755–13772, 2014.

[2] M. Fingas, *Handbook of Oil Spill Science and Technology*. Hoboken, NJ, USA: Wiley, 2015.

[3] C. Brekke and A. Solberg, "Oil spill detection by satellite remote sensing," *Remote Sens. Environ.*, vol. 95, no. 1, pp. 1–13, 2005.

[4] A. H. S. Solberg, G. Storvik, R. Solberg, and E. Volden, "Automatic detection of oil spills in ERS SAR images," *IEEE Trans. Geosci. Remote Sens.*, vol. 37, no. 4, pp. 1916–1924, Jul. 1999.

[5] J. Lu, "Marine oil spill detection, statistics and mapping with ERS SAR imagery in south-east Asia," *Int. J. Remote Sens.*, vol. 24, no. 15, pp. 3013–3032, 2003.

[6] C. Hu *et al.*, "MODIS detects oil spills in lake Maracaibo, Venezuela," *EOS, Trans., Amer. Geophys. Union*, vol. 84, no. 33, pp. 313–319, 2003.

[7] B. Bulgarelli and S. Djavidnia, "On MODIS retrieval of oil spill spectral properties in the marine environment," *IEEE Geosci. Remote Sens. Lett.*, vol. 9, no. 3, pp. 398–402, May 2012.

[8] A. Pisano, F. Bignami, and R. Santoleri, "Oil spill detection in glint-contaminated near-infrared MODIS imagery," *Remote Sens.*, vol. 7, no. 1, pp. 1112–1134, 2015.

[9] M. Cococcioni, L. Corucci, A. Masini, F. Nardelli, "SVME: An ensemble of support vector machines for detecting oil spills from full resolution MODIS images," *Ocean Dyn.*, vol. 62, no. 3, pp. 449–467, 2012.

[10] W. Su, F. Su, Y. Du, "MODIS based spectral and texture integration oil spill detection method," *J. Geo-Inf. Sci.*, vol. 16, no. 2, pp. 299–306, 2014.

[11] S. Liu, L. Bruzzone, F. Bovolo, and P. Du, "Hierarchical unsupervised change detection in multitemporal hyperspectral images," *IEEE Trans. Geosci. Remote Sens.*, vol. 53, no. 1, pp. 244–260, Jan. 2015.

[12] Y. Zheng, H. Li, H. Gu, and H. Feng, "Research on the haze removal method and parallel implementation for HJ-1 satellite data," in *Proc. Int. Conf. Multimedia Technol.*, Ningbo, China, 2010, pp. 1–4.

[13] G. Moser and S. B. Serpico, "Generalized minimum-error thresholding for unsupervised change detection from SAR amplitude imagery," *IEEE Trans. Geosci. Remote Sens.*, vol. 44, no. 10, pp. 2972–2982, Oct. 2006.

[14] S. Liu, L. Bruzzone, F. Bovolo, M. Zanetti, and P. Du, "Sequential spectral change vector analysis for iteratively discovering and detecting multiple changes in hyperspectral images," *IEEE Trans. Geosci. Remote Sens.*, vol. 53, no. 8, pp. 4363–4378, Aug. 2015.

[15] F. Melgani and L. Bruzzone, "Classification of hyperspectral remote sensing images with support vector machines," *IEEE Trans. Geosci. Remote Sens.*, vol. 42, no. 8, pp. 1778–1790, Aug. 2004.

[16] C.-C. Chang and C.-J. Lin, "LIBSVM: A library for support vector machines," *ACM Trans. Intell. Syst. Technol.*, vol. 2, no. 3, pp. 27:1–27:27, 2011. [Online]. Available: http://www.csie.ntu.edu.tw/~cjlin/libsvm